AGU PUBLICATIONS

Water Resources Research

RESEARCH ARTICLE
10.1002/2014WR016786

Well integrity assessment under temperature and pressure stresses by a 1:1 scale wellbore experiment

J. C. Manceau[1], J. Tremosa[1], P. Audigane[1], C. Lerouge[1], F. Claret[1], Y. Lettry[2], T. Fierz[2], and C. Nussbaum[3]

[1]BRGM, Orléans, France, [2]SOLEXPERTS AG, Mönchaltorf, Switzerland, [3]SWISSTOPO, Wabern, Switzerland

Key Points:
- A new experiment is presented for well integrity assessment
- The effect of pressure and temperature stresses on well integrity is evaluated
- The observations are explained and discussed with flow and geochemical modeling

Supporting Information:
- Supporting Information S1

Correspondence to:
J. C. Manceau,
jc.manceau@brgm.fr

Citation:
Manceau, J. C., J. Tremosa, P. Audigane, C. Lerouge, F. Claret, Y. Lettry, T. Fierz, and C. Nussbaum (2015), Well integrity assessment under temperature and pressure stresses by a 1:1 scale wellbore experiment, *Water Resour. Res.*, *51*, doi:10.1002/2014WR016786.

Received 16 DEC 2014
Accepted 12 JUN 2015
Accepted article online 16 JUN 2015

Abstract A new in situ experiment is proposed for observing and understanding well integrity evolution, potentially due to changes that could occur during a well lifetime. The focus is put on temperature and pressure stresses. A small section of a well is reproduced at scale 1:1 in the Opalinus Clay formation, representative of a low permeable caprock formation (in Mont Terri Underground Rock Laboratory, Switzerland). The well-system behavior is characterized over time both by performing hydro-tests to quantify the hydraulic properties of the well and their evolution, and sampling the fluids to monitor the chemical composition and its changes. This paper presents the well integrity assessment under different imposed temperature (17–52°C) and pressure (10–28 bar) conditions. The results obtained in this study confirm the ability of the chosen design and observation scale to estimate the evolution of the well integrity over time, the characteristics of the flow along the well-system and the reasons of the observed evolution. In particular, the estimated effective well permeability is higher than cement or caprock intrinsic permeability, which suggest preferential flow pathways at interfaces especially at the very beginning of the experiment; the significant variations of the effective well permeability observed after setting pressure and temperature stresses indicate that operations could influence well integrity in similar proportions than the cementing process.

1. Introduction

Well integrity can be defined as the capacity of wells to maintain zonal isolation of geologic formations and prevent migration of fluids (native or injected) between those formations [*Crow et al*., 2010]. To ensure this isolation, the well casing and the host rock are bonded by a cement sheath; after abandonment, a cement plug is used to avoid upward migration within the casing. The safety and performance of most subsurface operations are dependent on well integrity, including that of active wells used for the operations or of existing wells abandoned after prior operations. Detailed reviews or best practices on well integrity have already been performed [see e.g., *IEA-GHG (IEA Greenhouse Gas R&D Program)*, 2009; *Zhang and Bachu*, 2011; *Nelson*, 1990].

Literature also exists on the different ways the isolation might be compromised. During the well construction, operational defects might be created. During the drilling, the caprock adjacent to the borehole can be damaged leading to potential fractures or other disturbances [*Gasda et al*., 2008; *Kupferschmied et al*., 2015]. Cementing process is also important and poor cement/caprock or cement/casing bonding might occur, in case of poor cement mixing or placement, or gas migration during cementing [*Zhang and Bachu*, 2011]. The well abandonment might as well lead to potential loss of internal isolation according the method and material used for the well plugging [*Watson and Bachu*, 2009]. During the active life of the well or after its abandonment, the pressure and temperature conditions might evolve according to the type of operations carried out, changing stress conditions, which might displace the casing, damage the cement sheath and lead to the loss of integrity of the cement sheath and of the bonding with the casing or the host rock [*Zhang and Bachu*, 2011]. The wellbore properties could also be modified through chemical interactions between the fluids and the casing/cement/formation materials, depending on the geochemical environment in place or induced by the operations.

The evolution of the well integrity during its lifetime is therefore a combination of several physical processes (hydrological, thermal, mechanical and chemical at least) on the different materials and elements comprised in the well close environment (formation, cement, casing, interfaces, annuli) [*IEA-GHG*, 2009].

A large fraction of the recent published studies on well integrity understanding has been done in the field of CO_2 geological storage. A large effort has been dedicated to the study of individual elements/materials, mostly on the CO_2-induced geochemical reactions. For instance, a significant amount of studies have recently been already carried out to characterize these interactions in the context of CO_2 geological storage (see e.g., *Kutchko et al*. [2007, 2008, 2009]; *Duguid and Scherer* [2010]; *Wigand et al*. [2009]; *Cao et al*. [2013] for cement reactivity or *Carey et al*. [2010] for casing corrosion). Some supplementary work has been focused on the interactions and/or evolution of flow occurring at the interfaces or defects between elements (for instance *Carey et al*. [2010] and *Bachu and Bennion* [2009] for the casing/cement interface; *Wigand et al*. [2009], *Sweatman et al*. [2009] and *Mason et al*. [2013] for the caprock/cement interface; *Huerta et al*. [2013] and *Luquot et al*. [2013] for cement fractures). Some field studies have assessed the consequences of the contact between wellbores and CO_2 in an EOR field [*Carey et al*., 2007] and at a natural CO_2 reservoir [*Crow et al*., 2010]. Considering the wellbore close environment, *Gasda et al*. [2008] proposed a methodology to evaluate the effective permeability of that damaged zone through a field pressure test. This test has been performed on existing wells and some values are proposed by *Crow et al*. [2010], *Duguid et al*. [2013], and *Hawkes and Gardner* [2013].

However, the combined quantification of the isolation provided by a well drilled within a low-permeable rock formation and of its evolution under different stresses in a realistic context remains an issue. In particular the variability of a well integrity and the quantitative influence of each contributing factor described above (drilling, cementing, operations, etc.) on this variability is an open question. To go beyond the state of the art, we present in this paper a new in situ experiment, carried out in an underground rock laboratory offering caprock-like geological conditions. The well drilling and completion, and the implementation of a specific instrumentation in such a lab enables the access to or the modifications of properties usually difficult to measure or control in the field, such as the assessment of the hydraulic conductivity of the well or the establishment of a pressure gradient along the well or of new temperature conditions. Our purpose is to follow the evolution of the integrity of a well, under different physico-chemical changes, similar to those a well might be subjected to. In this paper, the influence of temperature and pressure changes is investigated.

The remainder of this paper is organized as follows. Section 2 presents in detail the experimental design, the experimental plan and the achieved operations. The monitoring methods and results are then presented in sections 3 and 4 to describe and to understand respectively the hydraulic characteristics of the wellbore and the geochemical conditions and their changes. The last section 5 is dedicated to a discussion on the well integrity changes that have been observed since the beginning of the operations.

2. Design, Experimental Plan, and Experiment Update

2.1. Location of the Experiment and Design

The experiment is located in the Mont Terri Underground Rock Laboratory (St-Ursanne, Canton of Jura, North-Western Switzerland). The Mont Terri is an anticline of the Jura fold-and-thrust belt, which was folded during the late Miocene to Pliocene (from 10.5 to 3 Myr). The Mont Terri Underground Rock Laboratory is located in the Opalinus Clay (see Figure 1), a rock formation consisting mainly of incompetent, silty and sandy shales, deposited around 175 Myr (Aalenien/Toracian). Regional indications of the total thickness of the Opalinus Clay are rare; however, in the laboratory, a total thickness of 130 m has been encountered. The Opalinus Clay is considered as a reference caprock-like formation. It can be characterized as an overconsolidated shale formation (present overburden 300 m, estimated overburden in the past at least 1350 m) with 40–80% clay minerals and micas, 10–40% quartz, 5–40% calcite, 1–5% siderite, 0–1.7% pyrite and 0.1–0.5% organic carbon [*Bossart and Thury*, 2008]. The maximum temperature the Opalinus Clay has suffered reached 85°C during the Cretaceous burial [*Mazurek et al*., 2006]. Three different lithofacies have been observed in this formation [*Bossart and Thury*, 2008]: in the lower part a shaly facies, an interstratified sandy and shaly facies in the upper part and a sandy-limy facies in between. The experiment is carried out in the shaly facies of Opalinus Clay (borehole BCS-5).

To comply with the objective of the experiment explained in the introductory section, the following concept has been proposed (see concept on Figure 2a): a small section of a wellbore is reproduced in the Opalinus Clay at scale 1:1 (5.5″ casing and Ø198 mm borehole), using classical materials regarding oil and gas

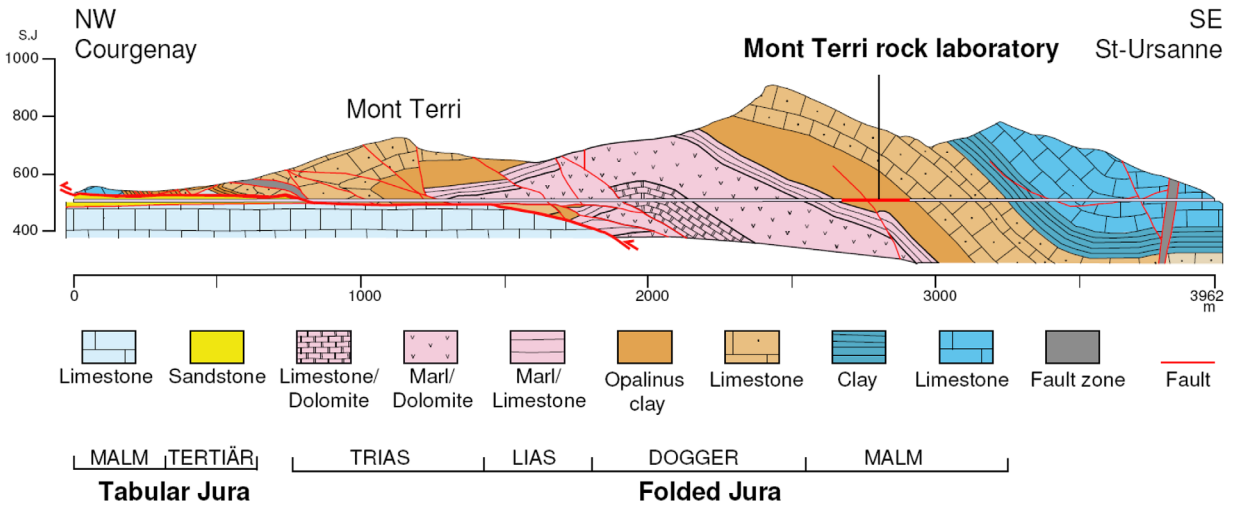

Figure 1. Geological cross section through the Mont Terri anticline including location of the Mont Terri Rock Laboratory (after *Bossart and Thury*, [2008]).

operations, i.e., carbon steel for the casing and class G cement with a water/cement ratio of 0.44. The system is divided in two parts: an internal part consisting of the casing and the cement plug inside the casing, and an external part behind casing consisting of the formation rock, the cement annulus and the casing. Three different intervals (i.e., a volume with no material) have been designed for a continuous monitoring

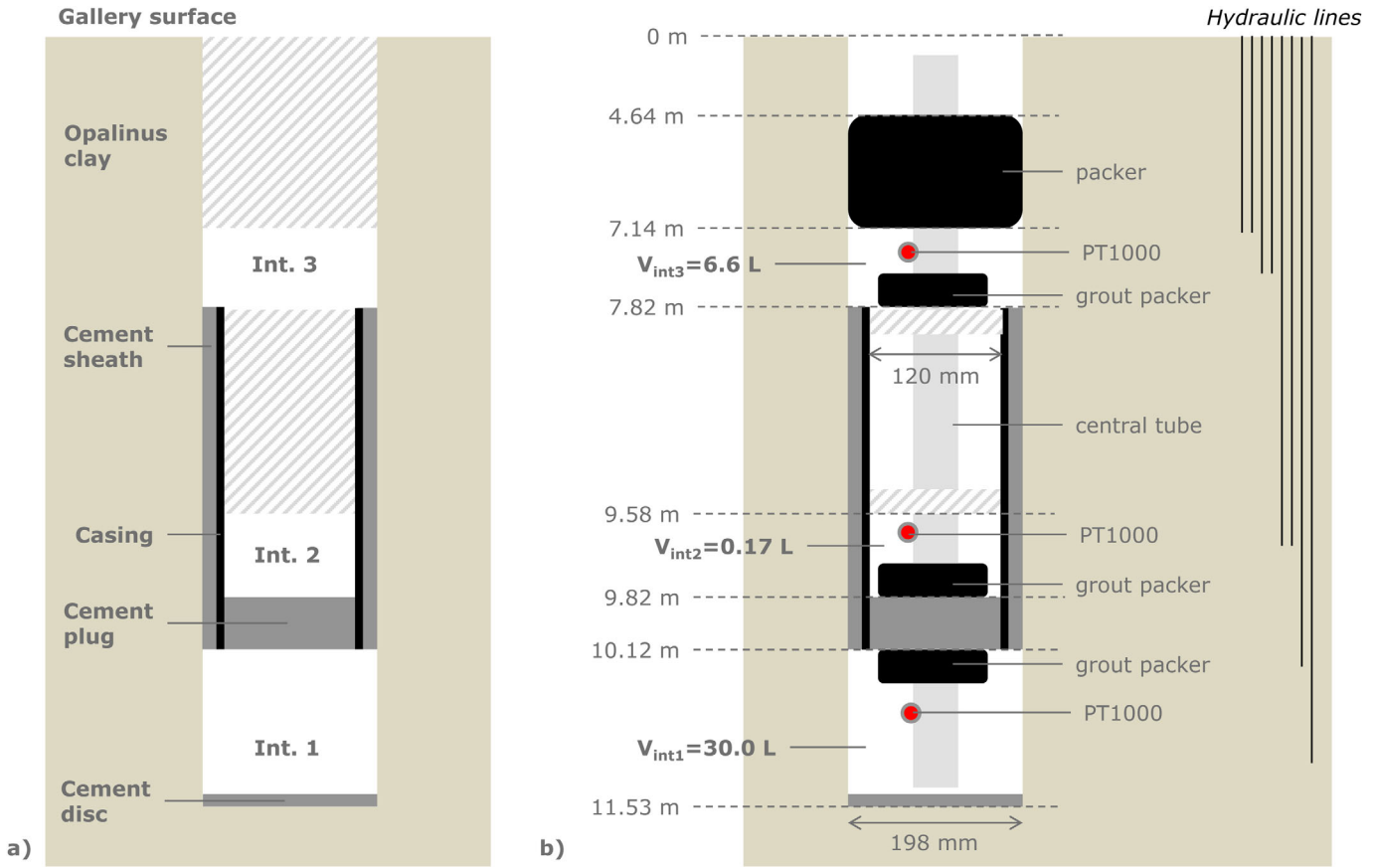

Figure 2. (a) Concept of the experimentation with the three observation intervals (not to scale). (b) Technical layout of the completion; only the hydraulic lines used for pressure monitoring, fluid extraction and injection are represented (not to scale).

of the pressure and temperature conditions. Fluid injection or extraction are also possible in those intervals, for controlling the intervals pressure and associated flowing rate through the well (i.e., in between these intervals) and for sampling the fluids for further fluid composition analyses. Interval 1 is located below the well-section, interval 2 over the cement plug, and interval 3 over the well-section (in contact with the external part of the casing). Temperature in interval 1 can be controlled, and therefore different temperature conditions can be set in the well.

From this concept, the completion has been designed as follows (see technical layout on Figure 2b). The well-section is 10.1 m deep and 2.3 m long: this depth has been chosen to make sure the well-system is not within the gallery excavation damaged zone (this may exist up to several meters depth with such galleries diameter); the system length has been chosen to facilitate an homogeneous grouting of the well-section.

A mechanical packer system and dedicated lines have been set-up to allow a proper cementing (both for the cement sheath and plug). Interval 1, located below the well elements, has a volume of 30 L approximately. It is equipped with two hydraulic lines, one with a port at the bottom of the interval and the second at the interval top. These lines are used for fluid injection/extraction and interval pressure monitoring at the surface with a pressure transducer. A PT1000 temperature sensor is also placed in the interval. Temperature control of this interval is possible by fluid circulation in a central stainless steel tube through hydraulic lines connected to a heater module at the surface. To stabilize the borehole wall and to protect the hydraulic lines from clogging, the interval is equipped with a filter (a slotted tube). A cement volume has been put at the very bottom of interval 1 (2 L, equivalent to a 65 mm height cement disc), to assess cement influence in interval 1. Interval 2 is located within the 5.5" casing above the cement plug and has a volume of 0.17 L approximately. It is equipped with two hydraulic lines, one with a port at the bottom and one at the top of the interval. Similarly than for interval 1, these lines can be used for fluid injection/extraction and pressure monitoring at the surface. The temperature is measured with a PT1000 probe. Interval 3 is located in the open borehole over the well elements and has a volume of approximately 6.6 L. It is equipped with one PT1000 temperature sensor and with 4 hydraulic lines, two in the upper part, and two in the lower part. These lines enable fluids (gases and/or aqueous solutions) to be efficiently sampled within the interval, and pressure to be measured at the surface. The isolation of the whole system from the surface is insured by a 2.5 m long packer, placed over interval 3.

At the surface, all lines coming from the borehole completion are connected to a control board (except the cement injection/extraction lines and the heater lines). A syringe pump (Teledyne Isco, model 500D) is used for the injection of both liquid and gas. The pump is remotely controlled (software DCAM developed by Solexperts) and the injection is possible at constant head or rate. A flow-controller module (Bronkhorst Thermal Mass Flow Meter, 0–10 g/h, 1–20 bar), also remotely controlled with DCAM, is used for the fluid extraction at constant rate. The heater module consists of a pressure reservoir equipped with a heating element and a pump connected to the hydraulic lines which controls heating fluid (boric acid) circulation within the central stainless steel tube of interval 1. Sampling can be performed from the interval lines at the control board using stainless steel sample vials (volume 40 ml). The data from all the sensors of the experiment are acquired with the system GeoMonitor, developed by Solexperts AG.

2.2. Experimental Test Plan and Achieved Operations

The operations described in this paper concern the borehole drilling, the system installation and the characterization (hydraulic and geochemical) of the system during one full year. The characterization was focused on the outside of the casing properties (interval 2 was finally not considered by the test plan, no connection between this interval and the rest of the system occurred). Temperature and pressure were modified during this period to address their influence.

Drilling of the borehole (borehole BCS-5) was done on 1 October 2012. It was followed by a borehole wall brushing (to increase the borehole roughness from the millimetre to the centimetre scale), a borehole deviation survey and a borehole video inspection. The drill core mapping report estimates the depth of the gallery excavation damaged zone (EDZ) to 60 cm, which indicates that the well-system should not be impacted significantly by this EDZ, being much below. The installation of the packer system was carried out on 4 October 2012. After connection of all lines to the control panel, function and tightness test were performed. No leaks were observed. After confirmation of the packer system functionality, the cement was prepared for the sections to be grouted (40 L water and 91 kg cement). Cement was injected through the

grout injection line until outflow of both overflow lines was noticed. To achieve a good cementation, cement circulation was continued for 20 min (injection in cement injection line, outflow out of upper over flow line). The grout packers were deflated the day after. The surface equipment was installed at the end of October 2012. During November and December 2012, the intervals were artificially saturated (the natural flow from the formation is very low compared to the significant volumes of the intervals). This was done using synthetic pore water (Pearson water, after *Pearson et al*. [2011]) representative of the Mont Terri pore water.

The hydraulic characterization of the system started in February 2013, with pressure tests performed at pressure values close to 10 bar. The temperature was then modified with a progressive heating up of the Interval 1 temperature in April 2013, from an initial temperature of 17°C up to 52°C; the maximum temperature was chosen to avoid any mechanical disruption of the Opalinus Clay formation. The heated system behavior was assessed between May and July 2013. The temperature change cycle was completed by a decrease of the interval 1 temperature set point to 46°C at the end of July 2013 and down to 31°C later in August 2013, with a system characterization between September 2013 and January 2014; during that period, the pressure was progressively increased up to 28 bar to observe the pressure influence.

3. Hydraulic Behavior of the Well-System

3.1. Methods

Hydro tests have been proposed in the literature [*Crow et al*., 2010; *Duguid et al*., 2013; *Hawkes and Gardner*, 2013]. They all assess the well integrity by using the concept of *effective well permeability* presented by *Gasda et al*. [2008], which is an indicator of the hydraulic conductivity of the well due to the numerous potential flowing paths that might exist. Concretely, the effective well permeability is computed as the cement annulus equivalent permeability if the total flow would occur homogeneously in this porous medium. In this experiment, the hydraulic monitoring set-up was developed in the aim of assessing this variable of interest, and its changes over time.

3.1.1. Hydro-Tests

Two types of tests have been performed in 2013. First of all, constant head injection tests (HI tests) were done at different times during the year. The principle is to increase the interval 1 pressure instantaneously and to observe the pressure response in interval 3. Even if these tests can be interpreted to retrieve the effective well permeability, they do not allow the continuous monitoring of the well integrity and some changes occurring between two different tests can be difficult to understand. Moreover, in our case, the intervals are in contact with the well but also with the surrounding clay, which might lead to some difficulties in interpreting the results of HI tests especially if the well integrity is important and the effective well permeability is low. A second approach (circulation steady state tests) is therefore additionally followed: the flow meter has been connected to interval 3 in order to impose a constant extraction flow rate in this interval, when no HI test is running. Simultaneously, a constant head injection is imposed in interval 1. The difference of pressure between interval 1 and interval 3 created by this setup is dependent on the effective well permeability among others – this procedure is to some extent similar to classical permeability measurements done on rock samples. The complete monitoring methodology enables to gather data during a large period, which both improves the well integrity changes detection and the results interpretation.

3.1.2. Model

To interpret the data, a 2D-radial numerical model was developed using TOUGH2 code [*Pruess et al*., 1999]. The model radial extension is 100 m, with 3901 cells. We use, in this model, the cement sheath permeability to represent the effective well permeability. The other influential input parameters are the caprock permeability, the intervals compressibility, and the boundary conditions in terms of pressure principally (caprock porosity and compressibility values have been taken close to their best estimate values in the laboratory provided by *Bossart and Thury* [2008], respectively 16% and 5E-10 Pa^{-1}). The intervals compressibility has been calculated independently over time, when water was injected in the intervals (during the HI tests mostly). The caprock permeability and pressure limit conditions have been inverted using the 2D-radial model during different recovery tests in the intervals (neither fluid injection nor extraction was performed) and are validated by the mass balance between the water injected and water extracted from the system. Knowing the intervals compressibility, the caprock permeability and pressure limit conditions at different time periods, the effective well permeability has been inverted during the pressure tests (HI tests and

circulation steady state). During those tests, the pressure in interval 1 and the extraction rate in interval 3 are fixed; this inversion has therefore been made with respect to the pressure in interval 3 and to the injected volume in interval 1. The details and results of the modeling procedure applied during the experimental campaign are presented in section 3.2.

3.2. Results

3.2.1. Monitoring Results

The observation year has been divided in three main periods with different temperature steps: Period 1 initial state at 17°C—March 2013, Period 2 52°C period—May–August 2013, and Period 3 31°C period—September 2013 to January 2014.

The data recorded and of interest are the pressures and temperatures in interval 1 and 3, as well as the injected and extracted volumes, respectively in interval 1 and 3. Figure 3 presents the data set for each of the measurement periods. During the first period, a very small difference of pressure ($<$0.05 bar, i.e., $<$5 kPa) between interval 1 and interval 3 occurred when the flow-meter was on (at 1 g/h, equivalent to ca. 1 mL/h), which is a sign of a good connection between the two intervals. The increase of interval 1 temperature up to 52°C before the second period lead to an increase of interval 3 temperature but at a lower value (the temperature stabilized at ca. 28°C), which means that a temperature gradient was induced in the system. With a water extraction rate similar to the first period, the pressure difference between the two intervals increased progressively from a ca. 0.1 bar to ca. 4 bar, which is a sign of a lowering of hydraulic conductivity between the two intervals. The interval 1 temperature was then decreased to 46°C at the end of the second period; after the stabilization of the pressure and temperature, the increase of the differential pressure between the two intervals continued, from 7 to 8 bar at an extraction rate of 1 g/h (1 mL/h).

Before the third observation period, the interval 1 was lowered to 31°C and the interval 3 stabilized at 22°C, and the pressure was imposed in both intervals at 11 bar. For a complete characterization of the system during this period, interval 1 pressure and the extraction rate were changed regularly (for the interval 1 pressure, different pressure plateau from 12 to 28 bar were set; for the extraction flow rate: no-extraction rate was set at the beginning followed with a small extraction rate – 0.16 g/h (0.16 mL/h)—to avoid a too high differential pressure between the two intervals).

In addition to the continuous monitoring data, Figure 3 also indicates the HI tests performed during the three observation periods; the results of these tests are all plotted on Figure 4. For an easier comparison between the different tests, the pressures recorded in interval 3 have been normalized according to the following formula: $P_{norm} = \frac{P(t)-P(t=0)}{P(t=end)-P(t=0)}$, where P_{norm} is the normalized pressure, P is the recorded pressure at different time, $t=0$ being the beginning of the test and $t=end$ being the end of the test when a constant pressure is reached in interval 3. It is important to note that for test d and e, the final equilibrium pressure could not be reached and has been estimated through the imposed pressure in interval 1. Nevertheless, tests a, b, c, d and e have been performed following the same protocol (i.e., shutting down the flow meter and increasing the interval 1 pressure). Figure 4 clearly displays a different pressure response form test to test, which slows down over time. This very first observation seems to confirm the increase of the well integrity over time observed through the continuous monitoring. Such HI tests were only performed during period 1 and 2 since the decrease in the hydraulic connection between the two intervals led to a too small response in interval 3.

3.2.2. Modeling Results

As mentioned in section 3.1, the intervals compressibility were estimated independently from the 2D-radial model. The interval 1 and 3 compressibility were calculated during period 1 at each HI tests knowing the injected volume and the associated increase in pressure in the two intervals: $\beta_c = \frac{V_{inj}}{V_c \, \Delta P}$, where β_c is the interval compressibility, V_{inj} is the volume injected in the total interval volume V_c to induce a pressure change ΔP. The HI tests being performed in interval 1, the compressibility of this interval can be obtained rather precisely. The compressibility of interval 3 is estimated during tests a and b according to its own pressure buildup; the pressure buildup being very rapid for those tests, this estimation is considered reliable despite the water was not injected directly in interval 3. However, during this time period, some of the injected water flows in the caprock. To avoid a too significant overestimation of the compressibility, the trend in the injected volume (after the test was completed) was removed for the calculation. For period 2, the interval 1 compressibility was computed from the water injected during test c, d and e. However, some issues with

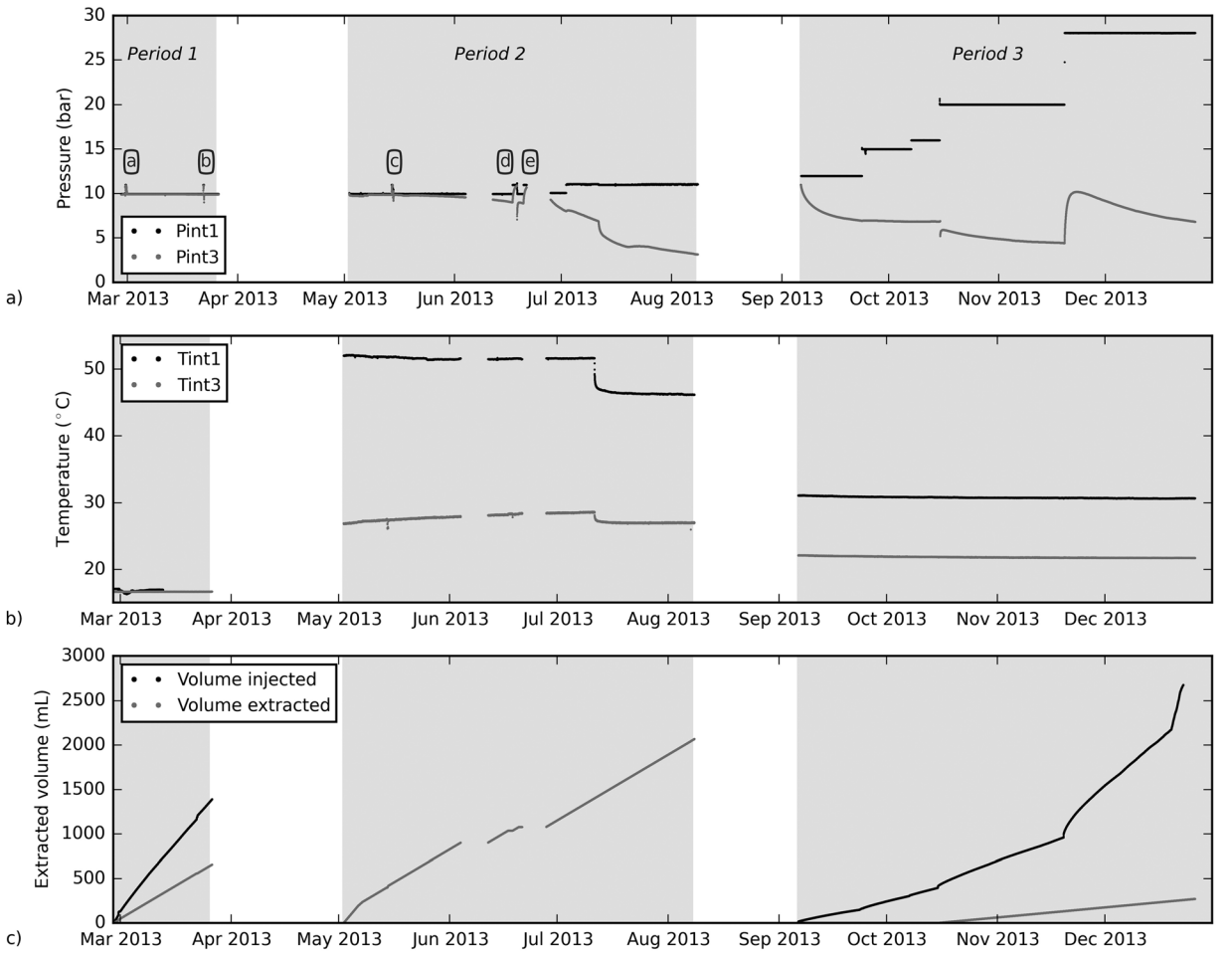

Figure 3. Raw data recorded during the first year of the experiment—(a) intervals pressure (the circled letters represent the HI tests), (b) intervals temperature, (c) injected volume in interval 1 and extracted volume in interval 3 since the beginning of each period. The transitional P and T variations between two periods due to Tint1 changes are not represented on the figure (white areas).

the injected volume sensors and the decrease of the well permeability made difficult and nonreliable the estimation of the interval 3 compressibility from the data recorded during these tests. Instead, a pressure buildup was performed directly in interval 3 (to 11 bar, on the 8 August 2013), which allows the direct calculation of the compressibility. For period 3, the interval 1 compressibility was calculated after a pressure buildup to 28 bar (on the 19 November 2013). All the computed compressibility values are provided in the supporting information. Despite the changes in the experimental conditions, the interval compressibility appeared to be relatively stable. The high values obtained compared to the water compressibility (ca. 5E-10 Pa^{-1} for the range of pressure and temperature of the experiment) can be attributed to the equipment within each interval, which is a classical observation made during borehole pressure tests [see e.g., *Neuzil*, 1982]. For the modeling, 1.3E-09 Pa^{-1} was considered as the interval 1 compressibility for the three observation periods, 2.5E-08 Pa^{-1} as the interval 3 compressibility for period 1 and 2.1E-08 Pa^{-1} for period 2 and 3.

The effective well permeability was estimated during tests a and b with the model described in section 3.1. For both tests, the model outcomes fit the data for a value of 20 mD (2E-14 m^2) (see supporting information Figure S2). The initial values (first period) considered for the caprock permeability and pressure boundary conditions have been derived with the 2D-radial model from the recovery in pressure in both interval 1 and 3 observed before the starting of the water circulation, between 22 January and 2 February 2013 (14 days). It is important to note that the consideration of the effective well permeability concept in the model had some consequences: this concept is considered to mimic the behavior of the vertical connection between the two intervals, whatever the connection paths are. However, the horizontal flow (toward the caprock)

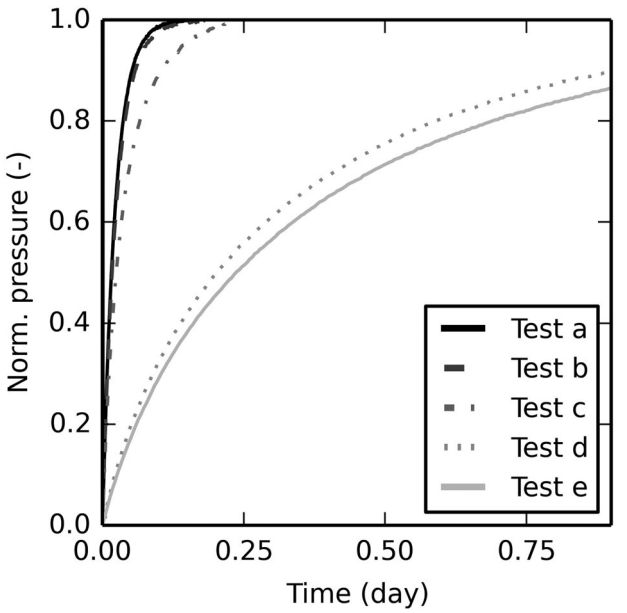

Figure 4. Normalized pressure in interval 3 during the HI tests (the normalized pressure is estimated for test d and e since the final equilibrium pressure was not reached during these tests).

would be different if the flow occurs through the cement matrix, through the cement/caprock interface or the cement/steel interface or even through specific fractures: the exchange surface between the flowing path and the caprock is indeed unknown. Tests a and b having shown a relatively high connection through the cement annulus, it has been decided to model period 1 considering the complete exchange surface between the cement annulus and the caprock. An homogeneous caprock permeability of 4E-5 mD (4E-20 m^2) has been estimated (see supporting information Figure S3). This value is consistent with the best estimate of the absolute permeability of the Mont Terri URL Opalinus Clay (2E-5 mD, i.e., 2E-20 m^2) [cf. *Bossart and Thury*, 2008].

The caprock permeability and effective well permeability values are also confirmed by the modeling of the circulation steady state tests during period 1 (constant pressure in interval 1 and constant extraction rate in interval 3). A good matching is obtained between the observations and the model results, both regarding the interval 3 pressure and the injected volume (see supporting information Figure S4).

For period 2, after 1 month of heating, the temperatures of the system were almost constant (52°C in interval 1, 28°C in interval 3). To reproduce the observations, isothermal simulations were performed considering in the model a vertical linear temperature gradient. However, this vertical linear temperature gradient does not represent the progressive temperature increase in the caprock formation and the induced increase in pressure. Moreover, during most of this period the data regarding the injected volume in interval 1 are considered not reliable since a leakage of the surface facilities has been found. However, during test c, the response of interval 3, in absolute pressure, reached a value slightly over the absolute pressure in interval 1, which indicates that some water was flowing from the caprock formation toward interval 3. Moreover, when the pump and the surface facilities were fixed, the pump had to extract some water to maintain a constant pressure in interval 1, at a low pace though (10 mL removed per day from the total 30 L). In summary, during period 2, the flow was directed from the caprock formation toward the well, but appears to be relatively low. In a first approach, given the difficulties to quantify more precisely this flow over the entire period, we decided to model period 2 considering a no-flow boundary between the well-system and the caprock. The consequence of this assumption is an overestimation of the effective well permeability.

The model results and the observations HI performed during this period match well with an effective well permeability of 5 mD (5E-15 m^2) for test c, 0.7 mD (7E-16 m^2) for test d and 0.6 mD (6E-16 m^2) for test e (see supporting information Figure S2). The increase in the well integrity after the increase in temperature is therefore confirmed by the quantification of the effective well permeability. The effective well permeability was also estimated from the long steady state tests in between each HI tests. The pressure of interval 3 decreasing continuously during period 2, the permeability decreases continuously and is estimated to 3 mD (3E-15 m^2) just before test c, to 0.33 mD (3.3E-16 m^2) just before test d and 0.28 mD (2.8E-16 m^2) just before test e and then decreases down to 0.042 mD (4.2E-17 m^2) at the end of period 2. In total a 3 orders of magnitude decrease of permeability has been assessed between period 1 and the end of period 2. Note that we also observe a slight increase of the permeability during each HI test.

The very low effective well permeability at the end of period 2 indicates that a far lower flow occurs through the cement annulus, indicating a potential closure of some flowing pathways. This decrease questions two assumptions made for period 1 modeling: the effective well permeability, initially considered

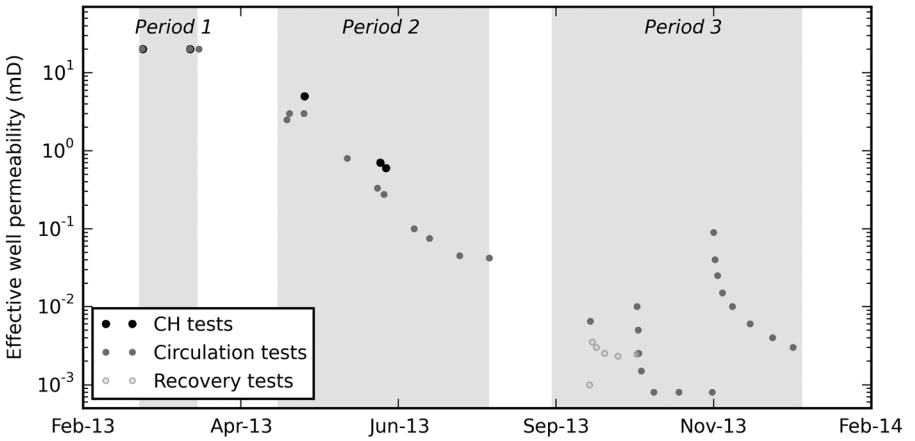

Figure 5. Estimated effective well permeability over time during year 1 of the experiment (the method of measurement is indicated).

homogeneous along the well, could have been decreased only at some locations; and the exchange area between the flowing pathways through cement annulus and the caprock, considered initially as the entire contact area between cement and clay, might have been decreased. We decided to keep the assumption of constant effective well permeability, as it is not possible to know precisely which parts of the cement annulus contribute to the observed low permeability. In addition, a no-flow boundary has been set between the cement annulus and the caprock and the equivalent permeability of the caprock at the interval 1 and interval 3 level is assessed at the very beginning of period 3. At that time, a constant pressure is imposed in interval 1 and the volume injected to keep this pressure is coherent with a caprock permeability at the interval 1 level of 3E-5 mD (3E-20 m^2). The respect of the mass balance during the rest of period 3 also confirms this value. The caprock permeability at the interval 3 level is estimated at a value of 1.5E-4 mD (1.5E-19 m^2) through the 2-D radial modeling of the recovery of interval 3 pressure (the pressure that was maintained at 11 bar was relaxed at the beginning of period 3 without any extraction rate imposed in interval 3). The caprock permeability at interval 1 level has therefore almost the same value than the homogeneous caprock permeability estimated for the first period (the slight decrease is likely to be due to the temperature difference between period 1 and 3), but for interval 3, the value is much higher (ca. 4 times higher). No physical reason seems to explain such an increase of permeability for interval 3: interval 1 has been subjected to highest temperature and pressure stresses without any consequences on the caprock permeability. The different way of inverting the caprock permeability between period 1 and 3 seems a more reasonable argument to explain this discrepancy. As explained above, the permeability calculated at the interval 1 and 3 level for the third period are equivalent permeability: they also account for the flow toward a potential part of the cement annulus with a high effective well permeability in contact with these intervals, which would allow a flow toward the caprock formation at the cement annulus/caprock interface. Considering that the wellbore caprock permeability is roughly homogeneous (reasonable assumption in this formation at that depth), a similar permeability found with the models used for period 1 and for period 3 would mean that the effective well permeability is very low at the interval level, while a difference would mean that a nonnegligible flow occurs toward the cement annulus: in our case, the results tend to show that the apparent decrease of effective well permeability does not occur homogeneously but rather in the lower part of the well. Considering these caprock equivalent permeability values, the effective well permeability value was estimated during the entire period: the associated pressure in interval 3 and the injected volume provided by the 2D-radial are given in the supporting information Figure S5 and appear to be in line with the observations. As a synthesis, Figure 5 recaps the estimations of the effective well permeability during the observation period. During period 3, three main pressure increases were performed (respectively of 3, 4 and 8 bar). For each of these pressure increases, the estimated effective well permeability appears to be increasing and then decreasing, meaning that the effective well permeability depends on the imposed pressure. This is a similar behavior (although in larger proportion) than for test c, d and e, where the increase in interval 1 pressure has led to an apparent increase in effective well permeability.

4. Chemistry of the well-system

4.1. Methods

The water filling the intervals 1 and 3 was sampled at different times during the observation period. Sampling was made using 40 mL stainless steel vials which are equipped with two-way valves at each side. The vials are connected to the interval lines and sampling was carried out by manually opening the interval line valves and letting the fluid enter. Before sampling, the vials were flushed with N_2(g) and set under vacuum to limit sample contamination by atmospheric gases. Interval 1 solution was sampled by opening the interval flow line and after purging the flow line of its volume. Solution from interval 3 was sampled after the flowmeter where the vial is progressively filled by the solution extracted from the interval.

Sampling vials were opened in a glove box under N_2 atmosphere (Jacomex GT Concept T4 with O_2 content between 0.1 and 5 ppm), to avoid any contact with the ambient air, where the solution was filtered (0.22 μm) and transferred to different aliquots. pH, Eh and alkalinity (by titration down to pH 2.4) were measured in the glove box. The Na, K, Ca, Mg, Fe and Si cations were analyzed by ICP/AES (Horiba-Jobin Yvon ultima 2), the Al and Sr cations by ICP/MS (Thermo seriX 2)), the Br, Cl, I, NO_3, SO_4, PO_4 and S_2O_3 anions by ionic chromatography (Thermo-Dionex ICS3000). The Fe^{2+} and S^{2-} speciations were analyzed by UV spectrometry (Varian Cary 50).

4.2. Results

4.2.1. Results of Chemical Analysis of Sampled Solutions

The evolution of the composition of the sampled waters in intervals 1 and 3 are reported in supporting information Table S6 and shown over time in Figure 6 for interval 3 and in the supporting information Figure S7 for interval 1, with the synthetic water used for intervals saturation as starting points. The pH is the parameter which presents the most significant variations with a decrease in Interval 1 from 7.6 to 6.7, followed by an increase up to a value of 8. In the Interval 3, the pH first increases to 7.9 and then decreases at a value of about 6.7. The other parameters show relatively little variations. The alkalinity increases and tends to stabilizes in both intervals, but at a higher value in the Interval 3. Ca and Mg have a similar trend in the two intervals with a decrease of their concentrations which then tend to stabilize. The sulfate concentration decreases in both intervals while the silica concentration increases.

4.2.2. Insights on the Well-System Given by the Recorded Chemical Evolution

Even little, the variations in chemical composition over time shown by the solutions sampled in Intervals 1 and 3 can be related to interaction or transport processes occurring in the well-system under study in the present in-situ experiment. Indeed, the synthetic water with a composition close to the Opalinus Clay pore-water which initially filled the interval can be subject to chemical changes because of the influence of two components: (i) the Opalinus Clay which surrounds the intervals (Figure 2); and (ii) the cement from the borehole annulus cement sheath, the cement plug in the completion and the cement disc at the borehole foot (Figure 2). Mixing processes can occur between the Opalinus Clay pore-water and the interval solutions by diffusion or advection. The water filling the intervals can also directly react with the clay rock at the borehole wall surface. The reaction of cement with water is expected to induce noticeable and fast changes with, in particular, an increase of the pH value. The composition of the water of the bottom interval (interval 1) can evolve to a cement water composition because of a diffusion and interaction in the cement disc and the water of the top interval (interval 3) because of the flow in the cement sheath, between the two intervals.

4.2.2.1. Thermodynamic and Mixing Modeling Approaches for the Interpretation of Sampling Water Evolution

A modeling approach based on thermodynamic and mixing processes was undertaken to evaluate these possible influences on the evolution of the water composition in the intervals 1 and 3. The thermodynamic models allow evaluating the composition of a water equilibrated with an infinite amount of Opalinus Clay or cement. The mixing models try to evaluate the water composition resulting from the flow between the intervals, the rock and the cement. The water composition expected to be at equilibrium with the Opalinus Clay minerals and with the cement phases was calculated for the different temperatures measured during the different periods. The solution at equilibrium with the Opalinus Clay was calculated by applying the model proposed by *Pearson et al*. [2011] which considers the equilibrium with a selection of Opalinus Clay forming minerals (calcite, dolomite, siderite, celestite, pyrite, illite(IMt2), chlorite(CCa2) and quartz) and cation exchange (involving Na, K, Ca, Mg, Fe, and Sr). This model was devoted to the simulation of the long-

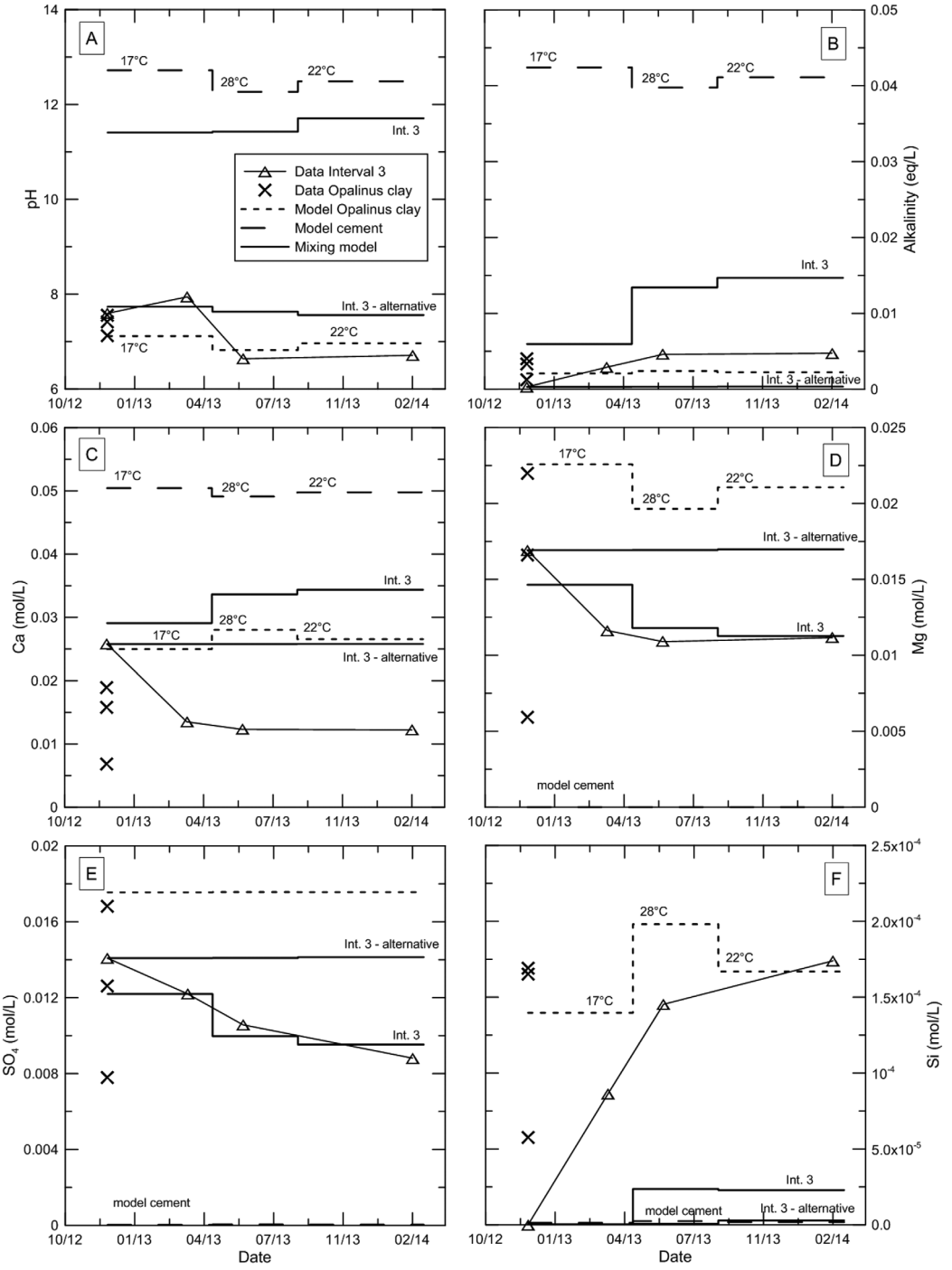

Figure 6. Interval 3 sampled water composition between November 2012 and February 2014, compared with Opalinus Clay pore water data, thermodynamic models results of Opalinus Clay water and cement water for the temperature conditions during the in situ experiment and mixing model results. (a) pH, (b) alkalinity and contents in (c) Ca, (d) Mg, (e) SO_4, and (f) Si.

term acquisition of the pore water composition by interaction with the rock [*Pearson et al.*, 2011]. For sake of simplicity, the same model was applied here for the different temperature conditions of the in situ experiment although the interaction between the Opalinus Clay and the water only took place during some months for each temperature condition and it is not likely to achieve the equilibrium with all the minerals considered in the model during this period. The effect of the cement on the water was evaluated by imposing an equilibrium between the Opalinus Clay pore water previously calculated and the expected phases of a Class G cement [*Gherardi and Audigane*, 2013]: CSH(1.6), portlandite, ettringite, hydrogarnets (C3AH6 and

C3FH6), hydrotalcite and calcite as a phase only allowed to precipitate. At the contrary to the model for calculating the Opalinus Clay pore water [*Pearson et al*., 2011], this model for the cement water has not been calibrated with experimental data. Then, the solution compositions obtained at different temperature with the cement model have only to be considered as indicative. In particular, no alkalis (Na_2O, K_2O) were considered in the model, which are sometimes introduced to adjust the solution pH in the cement curing steps [*Trotignon et al*., 2006].

A calculation which considers a mixing between different solutions was also made to consider the transport as a first approach in the experimental borehole system. The water calculated for each period for intervals 1 and 3 (W_{Int1} and W_{Int3}, respectively) can be expressed as follows:

$$W_{Int1} = mixf_{11} W_{Int1}^{period-1} + mixf_{12} W_{Opalinus} + mixf_{13} W_{cement} + mixf_{14} W_{synthetic} \quad (1)$$

$$W_{Int3} = mixf_{31} W_{Int3}^{period-1} + mixf_{32} W_{Opalinus} + mixf_{33} W_{cement} \quad (2)$$

where $W_{Opalinus}$, W_{cement} and $W_{synthetic}$ are the synthetic water and the waters calculated using the thermodynamic models for the Opalinus Clay and the cement. $W_{Int}^{period-1}$ is the water calculated for the same interval during the previous period of the experiment, or the synthetic water for the first period calculation. The mixing factors, which give the proportion of the different solutions forming the interval water, were obtained from measured data in the experiment (injected and extracted water volumes), from results of the hydraulic model (flow between the intervals and the borehole annulus and between the intervals and the rock) or were estimated (diffusion from the cement disc to the interval 1). The different mixing factors mimic the different transport processes identified in the experimental device: $mixf_{11}$ and $mixf_{31}$ are the proportions of water of the previous period remaining in interval 1 and interval 3, respectively; $mixf_{12}$ and $mixf_{32}$ correspond to the flow of Opalinus Clay pore-water entering in intervals 1 and 3; $mixf_{13}$ corresponds to the diffusive flow from the cement disc toward Interval 1; $mixf_{33}$ corresponds to the flow in the cement annulus toward Interval 3; and $mixf_{14}$ corresponds to the synthetic water injected in Interval 1.

Since the hydraulic model suggests that the flow in the cement annulus is more likely occurring channelized at the rock/cement interface than in the porosity of the cement, an alternative mixing model has been also tested to calculate the interval 3 solution composition by minimizing the effect of the cement on the resulting water. In this alternative model, the flow in the cement annulus toward the interval 3 obtained by the hydraulic model ($mixf_{33}$) is divided by an arbitrary coefficient and the remaining proportion of this flow is reported to a flow coming directly from interval 1. The calculation modifies as follows, for a flow divided by 1000:

$$W_{Int3-alternative} = mixf_{31} W_{Int3}^{period-1} + mixf_{32} W_{Opalinus} + \frac{mixf_{33}}{1000} W_{cement} + \left(mixf_{33} - \frac{mixf_{33}}{1000} \right) W_{Int1} \quad (3)$$

PHREEQC v3 geochemical calculation code [*Parkhurst and Appelo*, 2013] and the Thermoddem v2011 thermodynamic database [*Blanc et al*., 2012] were used for these numerical simulations.

4.2.2.2. Models Results and Implications on the Chemical Evolution

Together with the composition of the sampled waters in 3, Figure 6 shows the average Opalinus Clay pore water data sampled in boreholes PC-C, BWSA-1, BWSA-3 in Mont Terri URL (*Vinsot et al*. [2008]; *Pearson et al*. [2003]; and *Wersin et al*. [2009], reported in *Pearson et al*. [2011]). These three boreholes are in the same shaly facies than BCS-5 and are respectively 28, 47 and 127 m far from this borehole. Figure 6 also provides the results of the models calculating the water composition at equilibrium with the Opalinus Clay and the cement for the corresponding temperature over time and of the mixing model. This figure clearly indicates that the composition of the waters sampled during the experiment remains in the composition range of the Opalinus Clay pore water. The pore water data reported in the literature show the composition variability of a solution at equilibrium with the Opalinus Clay and this variability can, by itself, explain the observed changes of the water sampled in the intervals. The influence of the cement on the water composition appears as much weaker, with only the increase of the pH in the interval 3 in March 2013 and in the interval 1 in February 2014 which is perhaps related to a weak effect of the cement. The influence of the temperature on the calculated chemical composition is relatively low and such variations are few noticeable on the water analysis.

Solution compositions for interval 1 calculated using the mixing model present very little variations, at the exception of a decrease of the pH by 0.6 units. The calculation results are in the range of the measured data

and show a high influence of the injected synthetic water on the solution chemistry in interval 1. The influence of the cement water which diffuses from the cement disc is almost imperceptible, because of the large volume of the interval compared to the cement disc porosity. The first mixing model for Interval 3 is highly marked by the cement influence and the results are far from the analysis. Indeed, in this calculation all the water circulating in the borehole annulus toward the Interval 3 is considered to react with the cement. When the hypothesis of a flow occurring mainly at the interface without passing through the cement porosity is made (alternative model for interval 3), the mixing model can give results closer to the analysis. Some discrepancies are nevertheless obtained since the cations, sulfates and alkalinity are calculated by interval 1 model and interval 3 alternative model to remain almost constant and, consequently, do not reproduce the observed little increases or decreases.

Otherwise, the observed decrease of SO_4 content in intervals 1 and 3 could be explained by a bacterial activity in reductive conditions. Such a phenomenon is frequently observed in in situ experiments, where the water filling the borehole interval shows changes induced by sulfate-reductive bacteria [*Stroes-Gascoyne et al*., 2011; *Tournassat et al*., 2011].

5. Discussion on the Well-System Evolution

The effective well permeability has been shown to be dependent to pressure changes, especially during the end of period 2 and period 3, when it reached low values: the effective well permeability indeed increased when the pressure of interval 1 was built-up. This behavior is characteristic of fractured material, and in our case, this is likely to be the sign of flow occurring through microannuli rather than by the rock or cement matrix. This assumption can be reinforced by the relatively high initial effective well permeability (and more generally of the range estimated during the entire observation period, (2E-14 m^2; 8E-19 m^2)), which appeared to be incompatible with the absolute permeability expected for this type of cement (e.g., *Ghabezloo et al*. [2009] have measured permeability values between 1E-19 m^2 and 6.5E-20 m^2 for a class G cement). The large range of published effective well permeability values (7–80$\times 10^{-21}$ m^2 for *Hawkes and Gardner* [2013]; 5–10$\times 10^{-16}$ m^2 for *Crow et al*. [2010]; 2.5$\times 10^{-14}$ m^2 and 1.6$\times 10^{-13}$ m^2 for *Duguid et al*. [2013]) also suggests an important but variable role of preferential flow paths. Similarly, migration through interfaces has been observed, in the case of a 55 year-old oil well by *Carey et al*. [2007]. The results of geochemical modeling provided in section 4 are also in line with this assumption of flow through microannuli since the fluid composition of interval 3 does not match with a flow through the cemented matrix. In addition, it can be recalled that the hydraulic modeling shows a high exchange area between the well-section and the caprock formation, which is superior to the exchange area of both intervals. Considering the total well-system surface as exchange area during period 1, we have retrieved a caprock permeability value consistent with classical values in the Mont Terri URL (see section 3). This could indicate a localization of the flow (total or partial) at the caprock/cement interface. A flow occurring through micro-annuli within the Opalinus Clay formation is also conceivable. During drilling operations, stress redistribution and inelastic straining in the vicinity of the borehole may lead to the development of a borehole damaged zone. In the Mont Terri URL, shear and extensional fractures are typically observed within the EDZ [*Bossart et al*., 2002; *Marschall et al*., 2006, 2008; *Nussbaum et al*., 2011; *Yong et al*., 2013]. Kupferschmied et al. (2015) observed, with the resin impregnation technique, the same fracture network at the borehole scale.

A temperature dependence of the well integrity has also been suspected, with a dramatic decrease of the effective well permeability value, especially between period 1 (initial temperature) and period 2 (a temperature of 52°C was set at the bottom of the well-section). Interestingly, as explained in section 3 the flow modeling made for period 3 tends to show that the decrease in effective well permeability would be localized at the bottom of the well, and that the rest of the flowing pathways ensuring the flow during period 1 would be still in contact with interval 3. A very rough calculation, considering the equivalent caprock permeability at the interval 3 level obtained during period 3 (1.5E-19 m^2), a "real" caprock permeability equal to that calculated during period 1 (4E-20 m^2) and the geometry of the well-system (radius of 99 mm, length of interval 3 of 0.68 m), would lead to a "real" exchange length of $\frac{1.5\cdot 10^{-19} * 0.68}{4\cdot 10^{-20}} = 2.6\ m$: accounting for this value, the decrease of permeability would occur mostly in the lowest $2.30+0.68-2.55=0.4\ m$ of the well. This localization of the main decrease of permeability where the temperatures are the strongest would confirm that the temperature increase is the major cause of the permeability changes. Other reasons could nevertheless

be contemplated as natural or induced borehole convergence (including clay swelling). Indeed, a natural or induced convergence has been observed in many boreholes of the Mont Terri Rock Laboratory (*Labiouse and Vietor* [2014]). This can give rise to the collapse of these boreholes, especially in the shaly facies, which has a weak compressive strength. Therefore, such a convergence borehole convergence could also lead to a decrease of the thickness of the flowing paths.

The temperature induced decrease of the effective well permeability could be explained by thermal-hydraulic-mechanical (THM) effects [*Gens et al*., 2007; *Monfared et al*., 2014]. An additional 2D-radial model has been built, using TOUGH2 code, and similar to the one used in section 3 with, in addition, the steel casing in order to further assess the temperature changes during period 2. The increase in temperature of the system and surrounding formation during 4 months (duration of the second period) has been simulated. A linear gradient was set between interval 1 (52°C) and interval 3 (28°C) in the casing, which acts as a temperature source. Regarding the flowing properties, a constant pressure of 10 bar and a constant extraction rate of 1 g/h were set respectively in interval 1 and 3. The system properties estimated at the end of the first period (see section 3) were kept during the whole simulation. The simulations show that the radial temperature profile at the bottom of the well is not stable even in the close surrounding of the system and is continuously increasing. Using these results, the linear expansion potentially induced by the heating has been estimated: considering only the first meter from the well centre and considering respectively 1×10^{-5} °C^{-1}, 1.3×10^{-5} °C^{-1} and 1×10^{-5} °C^{-1} for the linear thermal expansion coefficient of cement, steel and clay (maximum value in *Bossart and Thury* [2008]), we can estimate the total linear expansion coefficient to 0.0949 mm after 1 month and 0.113 mm after 4 months of heating. In a first approach, to evaluate the potential hydraulic consequences of this expansion, the estimated value can be compared to the decrease of the distance between two perfect plans needed to obtain the changes in the effective well permeability observed after 1 month and 4 months of heating (i.e., decrease from 20 mD, down to 3 mD, and then to 0.04 mD). Considering the cubic law, this distance can be estimated with the following equation: $k \cdot S = \frac{L \cdot e^3}{12}$, where k and S are respectively the effective permeability of the well-system and the surface on which it is calculated; L is the length of the plans considered and e is the space in-between. If we consider that the flow is due to a space between the cement and the formation, L is calculated as the cement annulus external perimeter. This rough calculation gives a decrease in e of 0.0085 mm after 1 month, and a decrease of 0.016 mm after 4 months. These dimensions are even smaller than the estimated linear expansion but the computation is done for two perfect plans with no roughness and considers that the flow occurs on the whole interface. Despite these two assumptions that underestimate the value of e, this simple calculation shows that thermal expansion due to the increase in temperature might explain the decrease in hydraulic conductivity.

A clogging of the flowing pathways by the sedimentation of fine particles of clay minerals is another hypothesis that can be proposed to explain the decrease of the effective well permeability. Indeed, the retention of colloids in fracture planes is observed in laboratory and field experiments of colloid transport in fracture rocks of different natures [*Toran and Palumbo*, 1992]; *McKay et al*., 2000; *Mondal and Sleep*, 2012]. The flocculation, and then the transport and sedimentation, of clay colloids is favored with the temperature increase [*Baudracco and Aoubouazza*, 1995; *García-García et al*., 2006]. In sandstones, a permeability decrease with temperature increase due to a clogging by clay colloids has been evidenced by *Baudracco and Aoubouazza* [1995]. Then, the temperature increase during period 2 of the well integrity experiment should have enhanced a mobilization of clay minerals from the Opalinus Clay, followed by their sedimentation at the interface between the cement and the Opalinus Clay. However, the influence of such a clogging on the permeability can difficultly be quantified.

Even if a very limited part of the flow is likely to occur through the cement matrix and if the intervals water composition has been shown to be weakly influenced by the cement, the last hypothesis, which can be considered to explain the observed hydraulic conductivity decrease with the increase in temperature, is a mineral precipitation occurring at the bottom of the well. In order to test this hypothesis, the porosity changes due to the interactions between the cement and the fluid from interval 1 entering in the cement can be calculated for the three different temperature periods using the model previously established in section 4. The cement phases are destabilized by the solution from interval 1 and a thermodynamic equilibrium reaction give rise to a dissolution of portlandite and C3AH6 hydrogarnet while ettringite and hydrotalcite precipitate, as well as some calcite. The interaction of the cement with the solution from Interval 1 during the periods 1, 2 and 3 at 17°C, 52°C and 30°C, respectively, gives similar results in the three

calculation cases with a reduction of the porosity from 30% to about 29.9%. The influence of the temperature on this porosity reduction seems very scarce. Such a porosity decrease is not likely to induce a noticeable decrease of the permeability and, then, the hypothesis of a mineral precipitation is not relevant to explain the observed decrease in effective well permeability of about 4 orders of magnitude.

6. Summary and Conclusion

A new in situ experiment is proposed for following the evolution of a well integrity over time due to different changes, which could occur in its lifetime. The influence of changes of pressure and temperature conditions are investigated. A small section of a wellbore has been reproduced in the Opalinus Clay of the underground rock laboratory of Mont Terri, Switzerland (caprock-like formation) at scale 1:1. The initial state of the system has been characterized both hydraulically and chemically during one full year. Temperature and pressure have been modified during this period to address their influence. The paper presents the system, the methods that have been used, and the results of this observation period.

During that period, the isolation provided by a well barrier system has been observed and quantified at a realistic scale and under different stresses. Important insights from the experimental work have been derived: 1) the estimated effective well permeability is higher than cement or caprock intrinsic permeability, which suggest preferential flow pathways especially at the very beginning of the experiment; in addition, the fluid geochemical evolution and the pressure dependence of the well integrity confirm that assumption and indicate that the effective well permeability would be (partly or totally) due to the flow occurring at the interfaces between the caprock and the cement annulus. This supports the acknowledged importance of the cementing process. 2) the effective well permeability appears to be influenced significantly by the temperature and pressure stresses that have been set. The effective well permeability has drastically decreased after the temperature has been increased (the decrease of effective well permeability has been estimated to 3 orders of magnitude). Similarly, it has been increased to more than 2 orders of magnitude after an instantaneous pressure increase at the well bottom. The consequences of operations-induced stresses should then not be neglected, as they seem to influence the well integrity in similar proportions than the cementing process.

It should however be noted than the pressure and temperature variations investigated here (10 bar; 28 bar and 17°C; 52°C) cover a limited range of subsurface conditions. In addition, the caprock formation as well as the drilling and cementing processes are, by definition, specific to this very experiment. The generalization/upscaling of these observations should therefore be done with caution, as for most experimental works.

This experimentation will continue with a second observation period, dedicated to CO_2 geological storage issues. The same tests than those presented in this paper are planned replacing the pore-water with CO_2-rich pore-water. A sampling of the system is also planned at the end of the experiment to inspect the changes (notably mineralogical) on the different elements of the well.

Acknowledgments
The research leading to these results has been carried out in the framework of the ULTimate-CO_2 Project, funded by the European Commission's Seventh Framework Program (FP7/2007–2013) under grant agreement n° 281196. The ULTimate-CO_2 consortium would like to thank Swisstopo and Obayashi for funding a part of this experimentation. The authors wish to thank Laura Wasch (TNO) and Fabrizio Gherardi (IGG-CNR) for valuable discussions, and the three anonymous reviewers for their helpful comments. The data for this paper are available by contacting the corresponding author.

References

Bachu, S., and D. B. Bennion (2009), Experimental assessment of brine and/or CO_2 leakage through well cements at reservoir conditions, *Int. J. Greenhouse Gas Control*, *3*(4), 494–501.

Baudracco, J., and M. Aoubouazza (1995), Permeability variations in Berea and Vosges sandstone submitted to cyclic temperature percolation of saline fluids, *Geothermics*, *24*, 661–677.

Blanc, P., A. Lassin, P. Piantone, M. Azaroual, N. Jacquemet, A. Fabbri, and E. C. Gaucher (2012), Thermoddem: A geochemical database focused on low temperature water/rock interactions and waste materials, *Appl. Geochem.*, *27*, 2107–2116.

Bossart, P., and M. Thury (2008), Mont Terri Rock Laboratory Project, Programme 1996 to 2007 and Results, *Rep. Swiss Geol. Surv. 3*, Swiss Geological Survey (SGS), Wabern, Switzerland.

Bossart, P., P. M. Meier, A. Möri, T. Trick, and J. C. Mayor (2002), Geological and hydraulic characterization of the excavation disturbed zone in the Opalinus Clay of the Mont Terri Rock Laboratory, *Eng. Geol.*, *66*, 19–38.

Cao, P., Z. T. Karpyn, and L. Li (2013), Dynamic alterations in wellbore cement integrity due to geochemical reactions in CO_2-rich environments, *Water Resour. Res.*, *49*, 4465–4475, doi:10.1002/wrcr.20340.

Carey, J. W., M. Wigand, S. J. Chipera, G. WoldeGabriel, R. Pawar, P. C. Lichtner, S. C. Wehner, M. A. Raines, and G. D. Guthrie Jr. (2007), Analysis and performance of oil well cement with 30 years of CO_2 exposure from the SACROC unit, west Texas, U.S.A., *Int. J. Greenhouse Gas Control*, *1*(1), 75–85.

Carey, J. W., R. Svec, R. Grigg, J. Zhang, and W. Crow (2010), Experimental investigation of wellbore integrity and CO_2-brine flow along the casing-cement microannulus, *Int. J. Greenhouse Gas Control*, *4*, 272–282.

Crow, W., J. W. Carey, S. Gasda, D. B. Williams, and M. Celia (2010), Wellbore integrity analysis of a natural CO_2 producer, *Int. J. Greenhouse Gas Control*, *4*(2), 186–197.

Duguid, A., and G. W. Scherer (2010), Degradation of oilwell cement due to exposure to carbonated brine, *Int. J. Greenhouse Gas Control*, *4*(3), 546–560.
Duguid, A., R. Butscha, J. W. Carey, M. Celia, N. Chugunov, S. Gasda, T. S. Ramakrishnan, V. Stamp, and J. Wang (2013), Pre-injection baseline data collection to establish existing wellbore leakage properties, *Energy Procedia*, *37*, 5661−5672.
García-García, S., M. Jonsson, and S. Wold (2006), Temperature effect on the stability of bentonite colloids in water, *J. Colloid Interface Sci.*, *298*, 694–705.
Gasda, S. E., J. M. Nordbotten, and M. A. Celia (2008), Determining effective wellbore permeability from a field pressure test: A numerical analysis of detection limits, *Environ. Geol.*, *54*, 1207–1215.
Gens, A., J. Vaunat, B. Garitte, and Y. Wileveau (2007), In situ behaviour of a stiff layered clay subject to thermal loading: Observations and interpretation, *Géotechnique*, *57*, 207–228.
Ghabezloo, S., J. Sulem, and J. Saint-Marc (2009), Evaluation of a permeability-porosity relationship in a low permeability creeping material using a single transient test, *Int. J. Rock Mech. Mining Sci.*, *46*(4), 761–768.
Gherardi, F., and P. Audigane (2013), Modeling geochemical reactions in wellbore cement: Assessing pre-injection integrity in a site for CO_2 geological storage, *Greenhouse Gases Sci. Technol.*, *3*, 2152–3878.
Hawkes, C. D., and C. Gardner (2013), Pressure transient testing for assessment of wellbore integrity in the IEAGHG Weyburn–Midale CO_2 Monitoring and Storage Project, *Int. J. Greenhouse Gas Control*, *16S*, S50–S61.
Huerta, N. J., M. A. Hesse, S. L. Bryant, B. R. Strazisar, and C. L. Lopano (2013), Experimental evidence for self-limiting reactive flow through a fractured cement core: Implications for time-dependent wellbore leakage, *Environ. Sci. Technol.*, *47*, 269–275.
IEA-GHG (IEA Greenhouse Gas R&D Program) (2009), Long term integrity of CO_2 storage—Well abandonment, *Rep. 2009/08*, IEAGHG, Cheltenham, U. K.
Kupferschmied, N., K. M. Wild, F. Amann, C. Nussbaum, D. Jaeggi, and N. Badertscher (2014), Time-dependent fracture formation around a borehole in a clay shale, *Int. J. Rock Mech. Min.*, *77*, 105–114, doi:10.1016/j.ijrmms.2015.03.027.
Kutchko, B. G., B. R. Strazisar, D. A. Dzomback, G. W. Lowry, and N. Thaulow (2007), Degradation of well cement by CO_2 under geologic sequestration conditions, *Environ. Sci. Technol.*, *41* (12), 4787–4792.
Kutchko, B. G., B. R. Strazisar, G. V. Lowry, D. A. Dzombak, and N. Thaulow (2008), Rate of CO_2 attack on hydrated Class H well cement under geologic sequestration conditions, *Environ. Sci. Technol.*, *42*, 6237–6242.
Kutchko, B. G., B. R. Strazisar, N. Huerta, G. V. Lowry, D. A. Dzombak, and N. Thaulow (2009), CO_2 reaction with hydrated Class H well cement under geologic sequestration conditions: Effects of flyash admixtures, *Environ. Sci. Technol.*, *43*, 3947–3952.
Labiouse, V., and T. Vietor (2014), Laboratory and in situ simulation tests of the excavation damaged zone around galleries in Opalinus Clay, *Rock Mech. Rock Eng.*, *47*, 57–70.
Luquot, L., H. Abdoulghafour, and P. Gouze (2013), Hydro-dynamically controlled alteration of fractured Portland cements flowed by CO_2-rich brine, *Int. J. Greenhouse Gas Control*, *16*, 167–179.
Marschall, P., M. Distinguin, H. Shao, P. Bossart, C. Enachescu, and T. Trick (2006), Creation and evolution of damage zones around a micro-tunnel in a claystone formation of the Swiss Jura Mountains, paper SPE-98537-MS presented at International Symposium and Exhibition on Formation Damage Control, Lafayette, La, 15–17 Feb.
Marschall, P., T. Trick, G. W. Lanyon, J. Delay, and H. Shao (2008), Hydro-mechanical evolution of damaged zones around a microtunnel in a claystone formation of the Swiss Jura Mountains, paper ARMA-08-193 presented at 42nd U.S. Rock Mechanics Symposium (USRMS), San Francisco, Calif., 29 Jun-2 Jul.
Mason, H. E., W. L. Du Frane, S. D. C. Walsh, Z. Dai, S. Charnvanichborikarn, and S. A. Carroll (2013), Chemical and mechanical properties of wellbore cement altered by CO_2-rich brine using a multianalytical approach, *Environ. Sci. Technol.*, *47*, 1745–1752.
Mazurek, M., A. Hurford, and W. Leu (2006), Unravelling the multi-stage burial history of the Swiss Molasse Basin: Integration of apatite fission track, vitrinite reflectance and biomarker isomerisation analysis, *Basin Res.*, *18*, 27–50.
McKay, L. D., W. E. Sanford, and J. M. Strong (2000), Field-scale migration of colloidal tracers in a fractured shale saprolite, *Groundwater*, *38*, 139–147.
Mondal, P. K. and B. E. Sleep (2012), Colloid transport in dolomite rock fractures: Effects of fracture characteristics, specific discharge, and ionic strength, *Environ. Sci. Technol.*, *46*, 9987–9994.
Monfared, M., J. Sulem, P. Delage, and M. Mohajerani (2014), Temperature and damage impact on the permeability of Opalinus Clay, *Rock Mech. Rock Eng.*, *47*, 101–110.
Nelson, E. B. (1990), *Well Cementing*, Schlumberger Educ. Serv., Sugar Land, Tex.
Neuzil, C. E. (1982), On conducting the modified "slug" test in tight formations, *Water Resour. Res.*, *18*, 439–441.
Nussbaum, C., P. Bossart, F. Amann, and C. Aubourg (2011), Analysis of tectonic structures and excavation induced fractures in the Opalinus Clay, Mont Terri undergound rock laboratory (Switzerland), *Swiss J. Geosci.*, *104*, 187–210.
Parkhurst, D. L., and C. A. J. Appelo (2013), Description of input and examples for PHREEQC Version 3—A computer program for speciation, batch-reaction, one-dimensional transport, and inverse geochemical calculations, U.S. Geol. Surv. Tech. Methods, *Book 6, Chap. A43*, pp. 1–497.
Pearson, F. J., et al. (2003), *Mont Terri Project—Geochemistry of Water in the Opalinus Clay Formation at the Mont Terri Rock Laboratory, Geol. Ser. 5*, Federal Off. for Water and Geol., Bern.
Pearson, F. J., C. Tournassat, and E. Gaucher (2011), Biogeochemical processes in a clay formation in situ experiment: Part E—Equilibrium controls on chemistry of pore water from the Opalinus Clay, Mont Terri Underground Laboratory, Switzerland, *Appl. Geochem.*, *26*, 990–1008.
Pruess, K., C. M. Oldenburg, and G. J. Moridis (1999), TOUGH2 user's guide, version 2.0, *LBNL Rep. LBNL-43134*, Lawrence Berkeley National Laboratory, University of California, Berkeley, Calif.
Stroes-Gascoyne, S., C. Sergeant, A. Schippers, C. J. Hamon, S. Nèble, M. H. Vesvres, V. Barotti, S. Poulain, and C. Le Marrec (2011), Biogeochemical processes in a clay formation in situ experiment: Part D—Microbial analyses—Synthesis of results, *Appl. Geochem.*, *26*, 980–989.
Sweatman, R. E., A. Santra, D. S. Kulakofsky, and D. G. J. Clvert (2009), Effective zonal isolation for CO_2 sequestration wells, paper SPE-126226-MS presented at International Conference on CO_2 Capture, Storage, and Utilization, San Diego, Calif., 2–4 Nov.
Toran, L., and A. V. Palumbo (1992), Colloid transport through fractured and unfractured laboratory sand columns, *J. Contam. Hydrol.*, *9*, 289–303.
Tournassat, C., P. Alt-Epping, E. C. Gaucher, T. Gimmi, O. X. Leupin, and P. Wersin (2011), Biogeochemical processes in a clay formation in situ experiment: Part F—Reactive transport modelling, *Appl. Geochem.*, *26*, 1009–1022.
Trotignon, L., H. Peycelon, and X. Bourbon (2006), Comparison of performance of concrete barriers in a clayey geological medium, *Phys. Chem. Earth*, *31*, 610–617.

Vinsot, A., C. A. J. Appelo, C. Cailteau, S. Wechner, J. Pironon, P. De Donato, P. De Cannière, S. Mettler, P. Wersin, and H. E. Gäbler (2008), CO_2 data on gas and pore water sampled in situ in the Opalinus Clay at the Mont Terri rock laboratory. *Phys. Chem. Earth*, *33*, suppl. 1, S54–S60.

Watson, T. L., and S. Bachu (2009), Evaluation of the potential for gas and CO_2 leakage along wellbores, *SPE Drill Completion*, *24* (1), 115–126.

Wersin, P., E. Gaucher, T. Gimmi, O. Leupin, U. Mäder, F. J. Pearson, T. Thoenen, and C. Tournassat (2009), Geochemistry of pore waters in Opalinus Clay at Mont Terri: Experimental data and modelling, St-Ursanne, Switzerland, Mont Terri Project, *Tech. Rep. 2008-06*, Mont Terri Consortium, swisstopo, St-Ursanne, Switzerland.

Wigand, M., J. P. Kaszuba, J. W. Carey, and W. K. Hollis (2009), Geochemical effects of CO_2 sequestration on fractured wellbore cement at the cement/caprock interface, *Chem. Geol.*, *265*(1–2), 122–133.

Yong, S., P. K. Kaiser, and S. Loew (2013), Rock mass response ahead of an advancing face in faulted shale, *Int. J. Rock Mech. Min. Sci.*, *60*, 301–311.

Zhang, M., and S. Bachu (2011), Review of integrity of existing wells in relation to CO_2 geological storage: What do we know?, *Int. J. Greenhouse Gas Control*, *5*, 826−840.